quenching by the motional electric field of the faster atoms before they enter the interaction space. Aside from the relatively slow variation with magnetic field of the denominator of the formula for the life time[125] of the α-state, this type of quenching varies directly with H^2.

Although this technique for measurement of n does not give much accuracy, the results may be taken to provide some confirmation of the assumed velocity distribution. Fortunately, as previously discussed (Sec. 93), the only correction sensitive to the value of n is that due to motional Stark effect. Uncertainty in this has been estimated at 10 percent of the correction itself and has been included in the estimate of error of the results.

[125] See Part I, Eq. (42).

PHYSICAL REVIEW VOLUME 89, NUMBER 1 JANUARY 1, 1953

Fine Structure of the Hydrogen Atom. VI*†

EDWARD S. DAYHOFF,‡ SOL TRIEBWASSER,§ AND WILLIS E. LAMB, JR.‖
Radiation Laboratory, Columbia University, New York, New York

(Received September 15, 1952)

Measurements of improved accuracy of transition frequencies from the $2^2S_{\frac{1}{2}}(m=+\frac{1}{2})$ state to several of the $2^2P_{\frac{3}{2}}$ magnetic sub-states in deuterium are presented and analyzed. The shape of the observed resonance curves is discussed and compared with theory.

The experimental result is given for the $2^2P_{\frac{3}{2}}-2^2S_{\frac{1}{2}}$ separation, $\Delta E_D-\$_D=9912.59\pm0.10$ Mc/sec, for deuterium. This is combined with the result for $\$_D$ from the preceding article to obtain the $2^2P_{\frac{3}{2}}-2^2P_{\frac{1}{2}}$ separation, $\Delta E_D=10{,}971.59\pm0.20$ Mc/sec for deuterium. From ΔE_D and the auxiliary constants R_D and c a new value is computed for the fine structure constant $\alpha=1/(137.0365\pm0.0012)$. The uncertainty stated is considered to be a limit of error for our experimental procedure without allowance for the uncertainty of the auxiliary constants.

INTRODUCTION

THE preceding articles of this series[128] have discussed the theory of measurement of the fine structure of hydrogen and have presented highly accurate results for the $2^2S_{\frac{1}{2}}-2^2P_{\frac{1}{2}}$ shift $\$$ for hydrogen and deuterium. On the basis of the foundation already laid, measurements of improved accuracy of transition frequencies from the $2^2S_{\frac{1}{2}}(m=+\frac{1}{2})$ state to several of the $2^2P_{\frac{3}{2}}$ magnetic sub-states in deuterium are here discussed. The improved accuracy results mainly from improved magnetic field measurement technique, the elimination of some experimental corrections, and better stability of the equipment. The splitting of the levels in a magnetic field H is shown in Fig. 65 together with the nomenclature used for the sub-levels. The transitions reported here are indicated.

* Work supported jointly by the Signal Corps and ONR.

† Submitted by Edward S. Dayhoff in partial fulfillment of requirements for the degree of Doctor of Philosophy in the Faculty of Pure Science, Columbia University.

‡ Present address: Central Radio Propagation Laboratory, Microwave Standards Section, National Bureau of Standards, Washington, D. C.

§ Present address: Watson Scientific Computing Laboratory, Columbia University, New York, New York.

‖ Present address: Department of Physics, Stanford University, Stanford, California.

[128] W. E. Lamb, Jr., and R. C. Retherford, Part I, Phys. Rev. **79**, 549 (1950); Part II, Phys. Rev. **81**, 222 (1951); Part III, Phys. Rev. **85**, 259 (1952); Part IV, Phys. Rev. **86**, 1014 (1952); Triebwasser, Dayhoff, and Lamb, Part V, Phys. Rev. **89**, 98 (1953). Frequent references to these papers are made. Chapters, sections, figures, equations, tables, appendices, and footnotes of Part VI are numbered consecutively after those of Parts I through V.

W. GENERAL PROGRAM

An inspection of the day to day variations of the results[129] obtained with the metastable beam electric resonance apparatus[130] prior to about a year ago suggested the possibility of systematic errors whose effect was judged to be somewhat less than 1 Mc/sec in the final result. On the other hand, the internal consistency of individual runs appeared to indicate a possible precision approaching 0.1 Mc/sec in the result. It thus appeared that a systematic attack on residual inadequacies in the procedure was in order. On the one hand, empirical corrections of observations were reduced in number and simplified in application; on the other, the experimental parameters of the measurement were determined in an improved manner.

96. Improvements

The chief empirical correction to be removed was the relatively uncertain one[131] for "soft" component[132] of the metastable beam which required a great deal of time consuming computation. New interaction spaces with essentially complete polarization of the rf[133] relieved the problem of overlapping resonances, since nearby resonances which might overlap the desired one usually require a different polarization. By this

[129] See Part IV, Sec. 84 and, in particular, Table XVI.

[130] Described in detail in Part II.

[131] See Part IV, Sec. 73.

[132] Atoms in β-state. See Part I, Sec. 16.

[133] Described in Part V, Sec. 87.

means, the overlap corrections which were necessary in Part IV have been avoided in Parts V and VI. Additional computational work arising from variations of oscillator frequency and interaction space power level during the course of a run has been eliminated by use of an automatic frequency stabilizer[134] and a finely adjustable attenuator.

An incidental, though quite important, result of this program has been earlier availability of the results of runs after taking data. Thus malfunctioning of the equipment could be noticed quickly, changes in the apparatus could be evaluated rapidly, and the ability to undertake developmental experiments was increased.

The phase of the improvement program directed toward the experimental parameters bore fruit chiefly in connection with the magnetic field measurements. Several sources of error in the rotating search coil device used for field measurement were located and removed and a more reliable method of calibration for this device was found. These improvements, discussed below, are felt to account for the major part of the improved accuracy reported in Parts V and VI of this series.

Other improvements in the equipment whose effect was to increase the constancy of the metastable beam and to extend the time between cleanings are described in Appendices IX and X.

X. MAGNETIC FIELD MEASUREMENT

97. Method of Observation

The magnetic field measuring device is described in Sec. 39 of Part II. Two search coils are mounted on a single shaft rotating at 30 rps. One is in the field to be measured while the other rotates in the field of a permanent magnet. The emf's due to the two coils are combined in a bridge (Fig. 31, Part II) whose unbalance signal is amplified by a 30-cps narrow band amplifier. At balance, where the output of the amplifier is zero, the field of the electromagnet is given simply by

$$H = (\text{constant}) \times R, \tag{96a}$$

where H is the field to be measured and R is the total resistance in one arm of the bridge containing a variable resistance box. The calibration constant is a function of the number of turns and the area of the two search coils, the resistance of the fixed arm of the bridge, and the field strength of the permanent magnet. In the present measurements, it is about 1/65 gauss per ohm.

98. Corrections to Rotating Search Coil Readings

(a) *Effects of Temperature*

The search coil resistances of about 110 ohms (copper wire) had to be added to the bridge arm resistances. Their resistance variations with temperature were about 0.4 ohm per degree. Since it was difficult to measure the coil temperatures with sufficient accuracy, the box resistances were increased by a factor of about 10 over the values used for the measurements of Part IV, reducing possible error from this source from 0.06 to 0.006 gauss per degree. Hence calibrating both before and after the day's run avoided the need for measuring the temperatures of the coils as the error due to nonuniform heating was negligible.

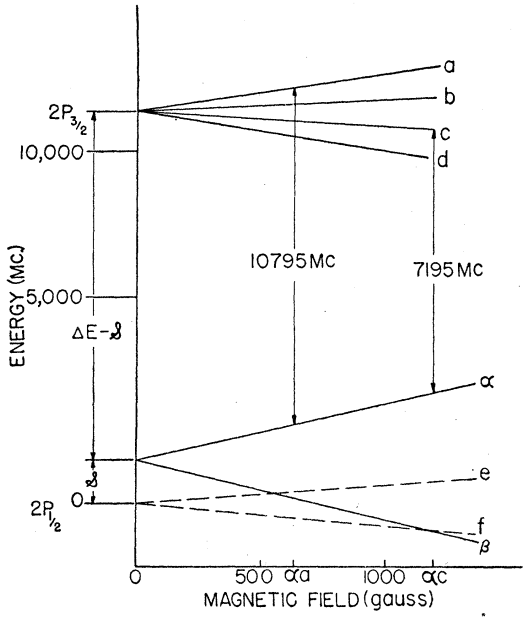

FIG. 65. Energy level splitting as a function of magnetic field for the $n=2$ levels of hydrogen, illustrating nomenclature of this paper and transitions reported.

Settings of the resistance box were standardized by intercomparison of the decade steps among themselves and with an external standard using a Wheatstone bridge arrangement with a sensitivity of a part in nearly 500 000 at a frequency near 30 cps. Repeating the measurements at several temperatures was sufficient to determine the temperature coefficients of the steps of the box. The absolute value of the standard resistance was unimportant since only ratios of resistances appeared in the results of the runs. The standard resistance and the resistance boxes contained low temperature coefficient precision resistors made by the General Radio Company. Their temperatures were monitored during runs with an accuracy sufficient to insure that error from this source would be less than one ohm.

It was found that the calibration constant depended on the temperature of the permanent magnet with a relative coefficient of 2.4×10^{-4} per degree. This variation was rather closely reproducible (Fig. 66) and results mainly from the reversible dependence of the magnetization of the permanent magnet on its temperature. Neglect of this is thought to be the most serious source of systematic error in the Part IV measurements

[134] See Appendix VIII.

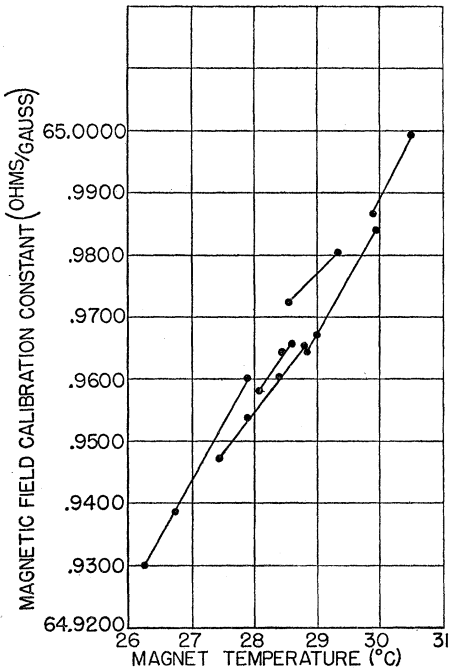

FIG. 66. Calibration constant of rotating search coil field measuring device as a function of temperature of the permanent reference magnet. Lines are drawn connecting points taken on the same day.

where the practice was to calibrate at the end of each day's run. The resultant errors were 0.25 Mc sec^{-1} $degree^{-1}$ for αe and 0.35 Mc sec^{-1} $degree^{-1}$ for αf. Since temperature in almost all cases increased nonuniformly several degrees during a run, the error would not be random. We have now thermally insulated the permanent magnet and improved the thermometry, greatly reducing the need for corrections. On most days on which runs were taken, the calibration constant was measured before and after the run. The magnet temperature was read at sufficiently frequent intervals to yield an average for each run accurate to 0.02 degree.

(*b*) *Effect of 60 cps Field Component*

It was observed that the calibration constant apparently depended on the relative phase of the 30-cps synchronous motor and the 60-cps power line. This dependence is associated with the 30-cps signal component generated in the search coil by a small 60-cps modulation of the magnetic field. Such 60-cps modulation is caused in our apparatus by the alternating currents used to heat the oven, bombarder cathode and plate heater. Equation (96a) is valid only if the 30-cps signals from the two coils are the induced emf's due to constant fields.

A loop of wire around a pole piece and fed from a variable amplitude source of 60-cps current was used to effect partial compensation of the field modulation of the electromagnet. In the runs of Part IV the degree of compensation was tested by observing the signal induced in an additional fixed coil placed nearby in the magnetic field. This method was later found to be inadequate, since the 60-cps component of the field was somewhat inhomogeneous. The error due to faulty compensation could easily have been 0.1 gauss at any magnetic field.

In the runs of Parts V and VI, the phase of the compensating field was made continuously adjustable and an improved test of the degree of compensation was developed. This test consisted of slipping the phase of the 4-pole, 30-cycle motor by 90 degrees (referred to the 60-cps power mains). Since the error due to the spurious 30-cps signal changes sign when this is done, adequate compensation existed when the above operation changed the balance point of the bridge less than ± 1 ohm in 80 000.

99. Calibration of Magnetic Field by $\alpha\beta$-Resonances

The calibration constant R/H is determined by observing the value of R for some known magnetic field H. The measurements of Part IV and the αc runs of Part VI used the sharp $\alpha\beta$-transition[135] for calibration. This is adequate when the π-polarization of rf electric field is used. Measurement at the βe crossing point (about 574 gauss and 1610 Mc/sec) then yields an accurate result. With the σ-polarization of rf electric field used in the αf, αa, and αc measurements, however, the situation is somewhat different and there is reason for expecting a genuine systematic disturbance of the resonance position.

The $\alpha\beta$-resonance as observed under these conditions (using the σ-polarized interaction space near the βe crossing point) is a second-order transition occurring both by way of the e state which is strongly coupled to the β-state by the motional Stark field and the f state which is coupled only by stray π-polarized fields. The f state, although far from resonance, is excited by the strong σ-radiation present while the e state, even though at exact resonance, is excited only by the π-polarized fringing rf fields of the interaction space and is relatively weak. Hence the observed $\alpha\beta$-resonance has a complicated shape, being a composite of the symmetrical e coupled shape and the very unsymmetrical f coupled shape.[136] The apparent center of the observed $\alpha\beta$-resonance is accordingly shifted from its expected position by an amount which depends critically on the stray fields in the interaction space. For this reason, the $\alpha\beta$-resonances are judged to be an unreliable method of calibration when observed with the σ-polarized interaction space. Experiments in which small electric fields which disturb the couplings of the various states are deliberately introduced show such shifts to be very real. As a result, it was decided that the proton reso-

[135] Theory in Chapter N of Part III.
[136] See Part II, Fig. 42; Part III, Fig. 52 and Chapter N.

nance[137] method of field calibration should be used for all precision measurements. Subsequent direct comparison of $\alpha\beta$- and proton resonances verified the highly variable nature of the $\alpha\beta$- with the σ-type interaction space. Differences of about 1 part in 10 000 sometimes were observed. These differences were of both signs, not randomly distributed, and usually showed drifts which apparently depended on the previous history of the apparatus. A group of $\alpha\beta$-runs could easily be in error by a part in 20 000. The π-type interaction space showed far less variation and better agreement between $\alpha\beta$- and proton calibration.

100. Calibration of Magnetic Field by Proton Resonance

A proton resonance probe was permanently mounted external to the vacuum envelope as near as possible to the interaction region. Resonances were observed near and corrected to 5.000 000 Mc/sec, for which $H = 1174.327 \pm 0.014$ gauss as computed from the results of Thomas, Driscoll, and Hipple.[138]

On four occasions when the vacuum system was opened for cleaning, a second probe was mounted in the center of the interaction region for the purpose of measuring the field inhomogeneity. The correction obtained on all occasions was 10 ± 1 parts in 80 000. A gradient of the strength of the magnetic field in the interaction space was found by moving the second probe along the path of the beam. The total field change in the interaction space was 12 parts in 80 000. Such a gradient might have required a correction to the mean field in the interaction space since the metastable beam was stronger on the entering side than on the exit side. This correction amounted to only $\frac{1}{2}$ part in 80 000 or

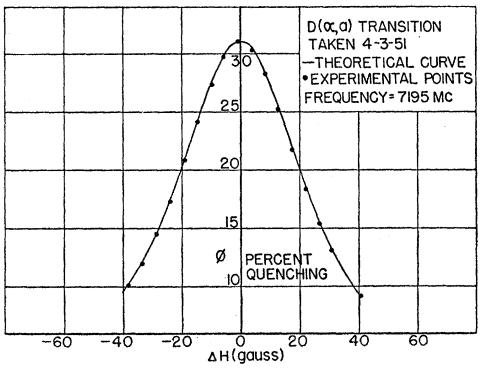

FIG. 67. Panoramic view of αa resonance curve. The abscissa is displacement from the resonant magnetic field $\bar{H}$ which is 630.68 gauss.

[137] R. V. Pound and W. D. Knight, Rev. Sci. Instr. **21**, 219 (1950).

[138] Thomas, Driscoll, and Hipple, J. Research Natl. Bur. Standards 44, 569 (1950). Cylindrical probes of $\frac{1}{4}$ in. diameter, $\frac{5}{16}$ in. long, with a 0.2 normal solution of copper sulfate were used. Corrections for paramagnetic ions and diamagnetism of water are sufficiently small to be neglected.

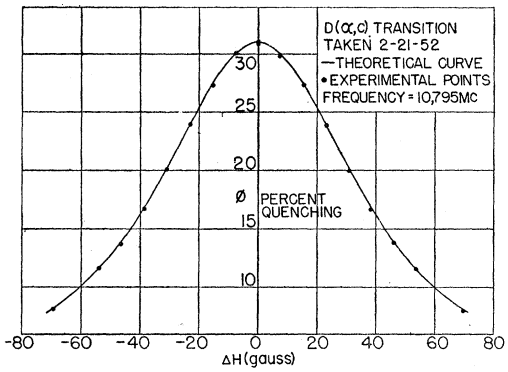

FIG. 68. Panoramic view of αc resonance curve. The abscissa is displacement from the resonant magnetic field $\bar{H}$ which is 1189.36 gauss.

0.006 Mc/sec for the αa transition with 20 percent quenching and was neglected.

To test the field measurement technique, calibrations were taken at 5.0 Mc/sec and 2.5 Mc/sec by zero-beating the proton resonance oscillator against a secondary standard at 5 Mc/sec in the former case and zero-beating its second harmonic against the same standard in the latter measurement. The ratio of resistance box readings with all corrections included was 2.0 to an accuracy of 1 part in 50,000. These two check points (1174 and 587 gauss) include about the full range of fields over which measurements in the experiment were made. To verify that the previous history of the iron was not significant, this test was done on two occasions with the same result. Additional evidence that effects due to the past history of the iron were negligible was provided by numerous measurements of the inhomogeneity correction mentioned in the paragraph above. In some cases deliberate efforts were made to induce irreversible changes in the inhomogeneity pattern (e.g., by reversing the field direction of the electromagnet), but in all cases the measured inhomogeneity was the same within expected error.

Y. LINE SHAPE

101. Panoramic Resonance Curves

Panoramic views of the αa and αc resonance curves are shown in Figs. 67 and 68. The αa transition was observed at 10,795 Mc/sec and the αc at 7195 Mc/sec, frequencies which center the αa at about 630 gauss (just above the crossing point of the β- and e states) and αc at about 1190 gauss (near the crossing field of the β- and f states). This choice of operating fields, together with the use of the low voltage quenching field[139] for the αc runs, insures that there will be no observable contribution to the quenching from atoms in the β-state. The solid lines labeled "theoretical

[139] Described in Part V, Sec. 85. A small π-polarized electric field will aid in quenching β-state atoms near the βf crossing point.

curve" are plots of the fractional quenching, ϕ:

$$\phi=\frac{\sum_m \int [1-\exp(-\psi_m/y)]y^2 \exp(-y^2)dy}{\sum_m \int y^2 \exp(-y^2)dy}, \quad (263)$$

where

$$\psi_m=\frac{Ab^2}{(\xi-a_m)^2+b^2}$$

gives the shape of the absorption line, and

$$\xi=\Delta H\cdot(dv/dH)_{AvH}$$

converts frequency differences into magnetic field differences with sufficient accuracy for use with the panoramics. Here the summations are over the hyperfine components, the integrations are over the velocity distribution, y is a dimensionless velocity variable $v/(2kT/M)^{\frac{1}{2}}$, a_m is the hyperfine energy of the mth hyperfine state in frequency units, and b represents the natural radiative width of the line as given by theory.[140] It is sufficiently accurate to use Eq. (263) as the various small asymmetries significant in the precision results cannot be seen on the scale of the panoramics.

102. Gross Fit and Slopes

The data are fitted to the theoretical curves by applying a power level correction to the quenching so that the value at the center of the line is exactly 31 percent for which the theoretical curves were calculated. The origin of abscissas is chosen so that the curve is symmetrically placed. The fit is as close as could reasonably be expected, considering the manner of taking data. Each experimental point is the result of just one measurement of beam quenching by the rf and quenching of the total beam by a strong dc field. In view of the closeness of this fit, and the smallness of corrections which depend on slope, the slopes used for calculating the precision data were taken from the theoretical curves and no direct measurements of them were made.[141]

TABLE XXIII. Observed line widths. The ratio of quenching at working points to quenching at peak is a measure of line width.

Run	$\phi_{w.p.}/\phi_{peak}$
Deuterium αa transition	
1	0.7079
2	0.7147
3	0.7101
4	0.7073
5	0.7065
6	0.7080
Mean	0.7091
Average deviation	0.0022
Theoretical	0.7128
Difference	0.0037
Deuterium αc transition	
10	0.6945
11	0.6940
12	0.6883
13	0.6930
14	0.6955
Mean	0.6930
Average deviation	0.0019
Theoretical	0.6972
Difference	0.0042

103. Line Width

A severe test of the quality of fit is provided by a close examination of the height of resonance curves at the "working points," using data obtained in the precision runs. The working points are two points chosen to lie approximately symmetrically above and below the apparent center of the resonance curve near its points of inflection. Thus, the ratio of the height of the curve at these points to the height at its center is a measure of the line width. This ratio, $\phi_{w.p.}/\phi_{peak}$, taken from the data of the precision runs is listed in Table XXIII. For the αa runs, the data indicate a small discrepancy from the theoretical expectation by 0.37 percent of the central height of the resonance with an Av. dev. of 0.22 percent. The αc runs show a similar condition, the discrepancy being 0.42 percent with an Av. dev. of 0.19 percent. In both cases, the lines are narrower than expected. As seen below, this discrepancy is easily understood and the fit is felt to be quite satisfactory.

In general, all effects which could possibly result in asymmetries or shifts significant at the level of accuracy of the precision runs have been included in the "theoretical" line widths used in this section, but terms which could only affect the lines symmetrically by small amounts have been dropped in the interest of simplifying the calculations. An omitted term which is known to have an appreciable influence on the line width is the power sharpening effect discussed in Appendix IV of Part III. This term would produce a lowering of the quenching at the operating points by an amount estimated at about 0.3 percent, which brings the experimentally observed and predicted line widths into reasonable agreement.

The low frequency transitions reported in Part V show a similar but less marked narrowing. Differences in degree of narrowing for various transitions stem from differences in the rf power level needed in each case. The effective power level depends on the average time of interaction of the beam and on the magnitude of the quenching observed for each hyperfine component of the resonance. The σ-polarized interaction space probably has a significantly shorter interaction time for αa and αc than for αf observations due to changes in the mode pattern occasioned by the short wavelength, since the diameter of the interaction space is

[140] See Part III, Sec. 62.

[141] Measurements of the slopes of the low frequency transitions are reported in Part V, Sec. 91. There the measured slopes were found to agree with the theoretical values.

about half a wavelength at 10 000 Mc/sec. At the lower frequencies, the π-polarization interaction space undoubtedly has a more uniform field distribution over the length of the beam, and consequently a longer average interaction time than the σ-polarized one. In addition, the peak quenching for a single hyperfine component is greater than the peak quenching for the composite resonance since the composite resonance is normalized to a predetermined height at its center.

The magnitude of the observed sharpening is in rough agreement with estimates of the effect of power sharpening. This explanation is thus not proven but made quite plausible. Since no appreciable shifts or asymmetries are introduced by this effect,[142] no detailed investigation of the phenomenon was attempted.

Z. RESULTS

104. Nature of Data

The taking of data for these runs follows fairly closely the plan previously described.[143] Briefly, this may be summarized as follows: The transition αa and αc in deuterium were studied at frequencies of 10,795 Mc/sec and 7195 Mc/sec, respectively. For the αa case, near the βe crossing point, the absence of β-state metastables is guaranteed by the motional electric field quenching, avoiding the necessity for a β-component correction.[144] For the αc transitions, near the βf crossing point, a small π-polarized electric field is introduced between the bombarder and the interaction region to insure the quenching of residual β-state atoms.[145]

A listing of dates of the runs is made is Table XXIV. Between runs number 2 and 3 on $D(\alpha a)$, the apparatus was opened and given a thorough cleaning. The $D(\alpha c)$ runs 1 through 9 are omitted since improvements were then made in the magnetic field calibration. Calibration was accomplished by means of the $\alpha\beta$ transition for the D(αc) runs while the proton resonance was used for the D(αa) data.

Each run usually contained four comparisons of the fractional quenching at the working points. Each quenching comparison consisted of two measurements of the quenching at one working point and one measurement at the other working point. The temporal sequence of these measurements was such that uniform drifts of the rf power level and beam strength did not influence the result. Each measurement of the fractional quenching at a working point consisted of four measurements of the rf quenching and three measurements of the quenching produced by a dc field sufficiently strong to quench essentially all metastables. These measurements were so arranged in time as to have eliminated any influence of uniform drifts in strength of metastable beam over the period of time needed for observing the rf and dc quenching twice each (60 seconds). In addition, at the beginning and end of each run, the fractional quenching at the nominal middle point of the resonance was measured (6 measurements of rf and 4 of dc quenching) for the purpose of normalizing the data to 31 percent quenching at the middle, the figure used in all of the asymmetry and shift calculations. For the αa runs numbered 5 and 6, the fractional quenching at the middle was also measured three times during the run but each measurement contained only 4 rf and 3 dc quenching values. This procedure was suggested by the tendency of the calibration of the rf power monitor crystal to drift during the run due to temperature effects. In extreme cases, the peak quenching might change from 30 percent to 32 percent during the run even though the crystal current was kept constant by continual readjustment of an attenuator in the rf line. The oscillator frequency was in all cases essentially constant during the run due to the use of the frequency stabilizer described in Appendix IX.

TABLE XXIV. Dates of runs.

Run No.	$D(\alpha a)$ Date	Run No.	$D(\alpha c)$ Date
1	2/21/52	10	6/21/51
2	2/22	11	6/25
3	2/26	12	6/26
4	2/27	13	6/27
5	2/28	14	6/29
6	2/29		

For the αa runs, the calibration of the rotating search coil used for measurement of the magnetic field was made before and after the run by means of the proton resonance. It is estimated that the maximum error of this technique was not more than 1 part in 40,000. With each measurement of the proton resonance field, the error due to possibly faulty compensation of the 60 cycle/sec ac component of the magnetic field was checked and maintained below 1 part in 80,000. The resistances of the rotating search coils were measured at the end of each run.

For the αc runs, the calibration was accomplished by measuring the resonant field of the $\alpha\beta$ resonance either at the end or the beginning of the run. The resonance frequency was nominally 1610 Mc/sec in all cases and was measured in the manner described below. The resonant field for the $\alpha\beta$ resonances was determined by a technique similar to that applied to the runs themselves, i.e., the quenching at a selected working point on one side was repeatedly compared with that at a point on the other side of approximately equal quenching. The central field was then calculated from these data using a slope measured near one or both of the selected points. Because of the sharpness of these resonances, it was unnecessary to make more than 5 or 6 comparisons in rapid succession.

[142] See Part III, Appendix IV.
[143] See Part IV, Sec. 75.
[144] β-component corrections are discussed more fully in Part IV, Sec. 73.
[145] This technique is discussed more fully in Part V, Sec. 86 and an additional correction of the results required by its use is calculated in Part V, Sec. 93, Eq. (258).

TABLE XXV. Summary of central fields.

Run	$\bar{H}$ gauss	Av. dev.	Residual	No. of items	Relative weight
Transition D(αa) (10,795.000 Mc/sec)					
1	630.655	0.029	0.024	4	48
2	630.655	0.086	0.024	6	8
3	630.676	0.115	0.003	4	3
4	630.752	0.057	0.073	4	12
5	630.845	0.093	0.166	4	5
6	630.663	0.043	0.016	4	22
Mean	630.679	0.071	0.035		
Transition D(αc) (7195.000 Mc/sec)					
10	1189.449	0.05	0.065	7	28
11	1189.275	0.06	0.109	4	11
12	1189.372	0.11	0.012	6	5
13	1189.308	0.08	0.076	6	9
14	1189.415	0.14	0.031	8	4
Mean	1189.362	0.080	0.068		

The use of the $\alpha\beta$ resonance taken with the σ-polarized interaction space, however, introduced the previously discussed possibility of systematic errors in the field calibration. In addition, at the time the αc runs were taken, the technique used for adjusting compensation of the 60-cps component of the magnetic field was somewhat defective, leading to an additional error, probably somewhat nonrandom in nature, perhaps as large as 5 parts in 80 000.

The following auxiliary data were collected in connection with each run: The frequency of beat note between the power oscillator and the appropriate harmonic of the crystal controlled secondary frequency standard was measured to about 0.001 Mc/sec by means of a calibrated auxiliary receiver. The frequency of the secondary standard was compared at the 5 Mc/sec level with the primary standard of frequency of this Laboratory to an accuracy no poorer than 5 cycles/sec. This primary standard of frequency was known to agree with the 5 Mc/sec broadcasts of the National Bureau of Standards to within 1 cps during all runs.

The temperature of the permanent reference magnet of the rotating search coil, read to 0.02°, was recorded after every two or three lines of data. The temperatures of the variable and fixed arms of the bridge of the rotating search coil, read to 0.1°, were recorded as needed, depending on their drift rates. Other information relating to the operating conditions and performance of the apparatus was recorded although not required in the analysis of the precision data.

105. Calculation of Central Fields

A preliminary value for the resistance corresponding to the central magnetic field of the resonance was obtained from Eq. (252).[146]

$$\bar{R}=\tfrac{1}{2}(R_a+R_b)+\tfrac{1}{2}(\bar{\phi}_b-\bar{\phi}_a)/|d\phi/dR|. \quad (252)$$

Here R_a and R_b are the true resistances in the variable bridge arm for the working points at the mean temperature of the run, including adjustment for the temperature drift of the fixed resistance arm. The second term corrects for the unavoidable slight asymmetry of placement of the working points about the center of the resonance and seldom amounts to more than about 10 ohms out of 40 000 (80 000 for αc). In calculating $\bar{\phi}_b-\bar{\phi}_a$, the quenching at one of the two working points was obtained by averaging successive pairs of measurements so as to eliminate effects of uniform power drift. The slope $d\phi/dR$ was obtained from the calculated radiative line shape. To this preliminary $\bar{R}$ was added a correction for the measured difference between primary and secondary standards of frequency and for the day to day changes in the difference between the power oscillator frequency and the harmonics of the secondary standard. The αa results were corrected to a true frequency of 10 795.000 Mc/sec and αc to 7195.000 Mc/sec.

The mean temperatures of permanent magnet and resistance boxes during the run were calculated and the calibration data adjusted to these temperatures. With the αa runs, a linear interpolation between the proton resonance resistances before and after the run was made to obtain the proton resonance resistance at the mean temperature of the permanent magnet for the run.

A frequency correction was applied, since the proton resonance oscillator frequency was measured by comparison with the secondary frequency standard. An additional correction to the proton resonance field because of the inhomogeneity of the magnetic field and the spatial separation of the proton probe and the interaction space was included. With the αc runs, the $\alpha\beta$-transition was used for calibration either before or after the run and adjustment to the mean temperature of the run was made by means of previously measured average temperature coefficients.

The magnetic field of the line center was then obtained by dividing the resistance of the corrected center by R/H, the number of ohms per gauss obtained from the corrected calibration resonance resistance and field. The αa and αc central fields are listed by runs in Table XXV. That table gives for each run the central field of the resonance for the frequency indicated, the average of the deviations of individual determinations within the run, the residuals of all runs with respect to

TABLE XXVI. Summary of corrections to observed $\Delta E_D-\mathcal{S}_D$. Units are Mc/sec.

Source of asymmetry or shift	Correction D(αa)	Correction D(αc)	Explanation section No.
Matrix element variation	0	−0.157	63
Quenching asymmetry	−0.038	−0.001	64
Incomplete Back-Goudsmit	0.138	0.077	65
Zeeman curvature	0	−0.015	65
Stark effect shift	0.005	0.005	57
Low voltage quenching field asymmetry	Not used	−0.005	86, 92
Total	0.105	−0.096	

[146] See Part IV, Sec. 77.

their mean, the number of separate determinations comprising each run, and the relative weight assigned to each run in calculating the means. Weights assigned to the various runs are in proportion to the number of determinations in the run divided by the square of the internal Av. dev. of the run.

An inspection of Table XXV shows that for the αa transition the average of the residuals is roughly equal to the mean Av. dev. divided by the square root of the number of determinations in a run. This situation is consistent with an assumption of general randomness in the errors causing the scatter and effective absence of day to day fluctuations other than those represented by the internal Av. dev.'s of the runs. For the αc results, the approximate equality of the mean Av. dev. and the average residual may be taken to indicate the presence of large day-to-day fluctuations.

106. Asymmetry and Shift Corrections

Corrections to the apparent position of the resonance have already received extensive treatment in these articles and need not be repeated in detail. For the transitions reported here, some of the corrections are considerably smaller than for transitions previously reported, the total amounting to -0.096 Mc/sec for the case of D(αc) and $+0.105$ Mc/sec for D(αa). Individual corrections are listed in Table XXVI.

It will be noted from the table that both the matrix element variation and the Zeeman curvature corrections are zero for the αa transition. This derives from the fact that the a state (for which $m=+\frac{3}{2}$) is not mixed with any other state by the Zeeman coupling. The low voltage field quenching asymmetry correction is required for the αc runs only.

107. Results

The observed positions of the resonances listed in Table XXV can be converted into values of the quantity $\Delta E_D - \mathcal{S}_D$ by use of the Zeeman effect formulae (164–172).[147] After applying the corrections listed in Table XXVI, the final results for $\Delta E_D - \mathcal{S}_D$ are in Table XXVII, 9912.59 Mc/sec from D(αa) and 9912.80 Mc/sec from D(αc).

The difference between the D(αa) and D(αc) results is 0.21 Mc/sec. This discrepancy is comparable to the mean average deviation of the D(αc) run results. It does not seem likely that its origin is to be found entirely or predominantly in fluctuations of a random nature since it is three times the sum of the technical probable errors of the αa and αc results. It is felt that this discrepancy is to be ascribed to systematic error arising in the $\alpha\beta$-resonance method of field calibration used for the αc runs. Reasons for expecting such a difficulty are set forth in Sec. 99 where it is indicated that an error of 1 part in 20 000 is likely. An error in the magnetic field of this magnitude amounts to 0.14 Mc/sec for $\Delta E_D - \mathcal{S}_D$ which can quite satisfactorily account for the discrepancy. In view of this situation, it is felt that the αa runs alone should be used to obtain a final value for $\Delta E_D - \mathcal{S}_D$.

[147] See Part III, Sec. 55.

TABLE XXVII. Summary of results.

	D(αa)	D(αc)	
Frequency	10 795.000	7195.000	Mc/sec
Magnetic field for resonance	630.679	1189.384	gauss
Preliminary $\Delta E_D - \mathcal{S}_D$	9912.489	9912.899	Mc/sec
Corrections, Table XXVI	+0.105	−0.096	Mc/sec
Final $\Delta E_D - \mathcal{S}_D$	9912.594	9912.803	Mc/sec
Mean residual	0.049	0.156	Mc/sec
Probable error	0.017	0.054	Mc/sec
Statistical limit of error (3 times probable error)	0.05	0.16	Mc/sec
Final limit of error estimate (see text)	0.10	···	Mc/sec

Reasons underlying the choice of operating conditions for the final high precision determination of $\Delta E_D - \mathcal{S}_D$ include the following: The slope of the αa transition is about 1.4 Mc sec^{-1} gauss^{-1} which together with the choice of an operating field of only 630 gauss makes the Zeeman energy reasonably small without broadening the resonance in magnetic field too much. There is no Zeeman curvature or variation of the matrix element for this transition, facts which could be of some consequence should some omission in the theory later be uncovered. The operating frequency is chosen so that there will be no contamination of the beam by β-component at the operating fields. These reasons singly are not compelling but taken together indicate the extent to which ideal measurement conditions could be chosen.

108. Limit of Error of Result

This work has aimed throughout at a 0.1 Mc/sec limit of error, and consequently effects making contributions to the experimental result of order 0.01 Mc/sec have been investigated. The statistical probable error of the result is 0.017 Mc/sec. An error of more than three times this or 0.05 Mc/sec has a chance of only one in 100. To arrive at a reasonable limit of error, one must add to this an estimate of possible remaining systematic errors which will be taken as 0.05 Mc/sec. This figure is equal to the mean day-to-day scatter of the αa results. A systematic error whose nonrandom day-to-day changes were significantly larger than this amount would have been noticed whereas smaller effects would have been masked by the scatter. (An example of such an error would be possibly some effect due to the presence of charged insulating layers which could form on the inner walls of the apparatus. Presumably effects of this sort would change continuously with time except when the apparatus was cleaned.) An unvarying systematic effect or an omission in the theory by which the experimental results are interpreted would presumably spoil the consistency of values derived from different transitions. It is felt that the mutual con-

sistency of the results reported in Part V bears out the general reliability of the theory and method at least to this order of accuracy. The figure of $\pm(0.05+0.05)$ or ± 0.10 Mc/sec is therefore adopted to represent the range within which the authors believe the true value to lie.

109. The Fine Structure Constant

When the value of δ_D, 1059.00±0.10 Mc/sec, reported in Part V is added to $\Delta E_D - \delta_D$, $\Delta E_D = 10{,}971.58 \pm 0.20$ Mc/sec is obtained. This quantity leads to a value for the fine structure constant when inserted into the well-founded theoretical expression[148] for the fine structure separation

$$\Delta E = \frac{1}{32}\mu\alpha^4 + \frac{5}{256}\alpha^6 + \frac{1}{32\pi}\alpha^5\left[1 - \frac{5.946}{\pi}\alpha\right]. \quad (135)$$

In ordinary units, for deuterium, this equation becomes

$$\nu_{\Delta E} = \frac{cR_D}{16}\alpha^2\left[1 + \tfrac{5}{8}\alpha^2 + \frac{\alpha}{\pi} - \frac{5.946}{\pi^2}\alpha^2\right]. \quad (264)$$

Actually, α is not determined from these measurements but rather the quantity $\alpha^2 cR_D$. For the auxiliary constants, the values $R_D = 109{,}707.44$ cm^{-1} and $c = 299{,}790.0$ km/sec given by Bearden and Watts[149] have been used. One obtains then $\alpha^{-1} = (137.0365 \pm 0.0012)$ for the value of the reciprocal of the fine structure constant as determined from the *fine structure* by this investigation.[150] The uncertainty quoted includes no allowance for uncertainty in the auxiliary constants. The uncertainty in c given by Bearden and Watts would add 0.0002 to the uncertainty in α^{-1}. A change in the value accepted for c by +1 km/sec would change α^{-1} by +0.00023.

It is of interest to compare this value with the most recently available value from measurements of the *hyperfine structure* of the ground state of hydrogen. Salpeter and Newcomb[151] discuss radiative corrections and find $\alpha^{-1} = (137.0355 \pm 0.0010)\cdot(1 + \frac{1}{2}\delta)$ where the quantity δ is inserted to take account of effects as yet uncalculated due to departure of the proton magnetic field from that of a point dipole. The uncertainty given is a probable error. The value of δ may be greater than $\pm 2\times 10^{-5}$ according to Salpeter and Newcomb and consequently the small difference between their value and ours cannot be taken seriously at the present time. It should be noted that the comparison is not affected by the values used for the auxiliary constants.

The authors have benefited greatly from many valuable discussions of the theoretical aspects of this work with Professor N. M. Kroll. We wish to thank the members of the Columbia Radiation Laboratory staff for their wholehearted cooperation, and especially Messrs. J. Heberle and H. Reich for assistance with the taking of data, and Messrs. A. H. Barrett and R. Herman for assistance with the computation.

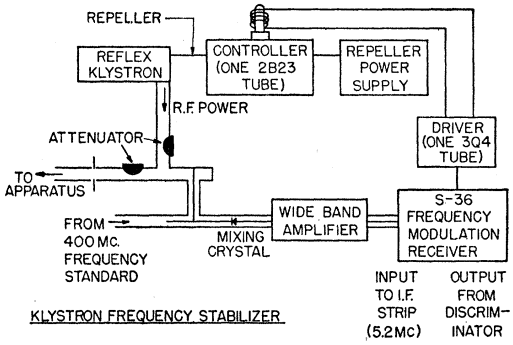

FIG. 69. Block diagram of frequency stabilizing arrangement used with reflex klystrons. The wide band amplifier is unnecessary when the beat note is strong.

APPENDIX VIII. OSCILLATOR FREQUENCY STABILIZER

Several of the reflex klystron oscillators showed rapid fluctuations in frequency of the order of several tenths of a megacycle. In addition to adding some degree of uncertainty to the frequency determination and requiring an extra set of corrections to the data, these fluctuations were reflected as power variations when the resonant interaction space was used. A block diagram of the frequency stabilizing arrangement constructed is shown in Fig. 69. The beat frequency between the Klystron and an appropriate harmonic of a crystal controlled standardized oscillator is amplified and used to provide an error signal to correct the Klystron frequency. The error signal is transferred to the dc level of the Klystron repeller by means of a 2B23 magnetically controlled diode.[152] The stabilization achieved in this way, even in the absence of additional dc amplification of the error signal, was adequate to confine the oscillator to a frequency band of width 5 kc/sec over a half-hour period.

APPENDIX IX. OVEN TEMPERATURE REGULATOR

Large fluctuations in beam size traceable to fluctuations in the temperature of the dissociating oven were observed on some occasions. Such fluctuations made it impossible to use the apparatus and since the cure for the source of the condition was usually replacement of the oven, which takes several days, a symptomatic cure in the form of a temperature regulator was tried. The regulator obtained its error signal from a photoelectric cell which monitored the light output of the hot oven. The amplified error signal was used to control

[148] See Part III, Sec. 53.
[149] J. A. Bearden and H. M. Watts, Phys. Rev. **81**, 73 (1951).
[150] Earlier results were reported as follows (Part IV): $\Delta E_D - \delta_D = 9912.40 \pm 1.0$ Mc/sec, $\Delta E_D = 10{,}972.11 \pm 1.0$ Mc/sec, $\alpha^{-1} = 137.033 \pm 0.006$.
[151] E. E. Salpeter and W. A. Newcomb, Phys. Rev. **87**, 150 (1952).
[152] E. S. Dayhoff, Rev. Sci. Instr. **22**, 1028 (1951).

a variable impedance device put between the oven and the voltage regulated power line. This arrangement was able to reduce abnormal beam fluctuations by a factor of 5 or more in cases where such fluctuations were really due to variations in oven temperature. It did not cause more than a slight improvement in the beam steadiness on "quiet" days.

APPENDIX X. DETECTOR IMPROVEMENTS

An attempt was made to increase the time between overhauls[153] by making it possible to heat the detector strongly on occasions when it appeared to have become poisoned. Heating to a bright orange color seemed to be quite successful in restoring the beam to its initial strength. Generally, this procedure was necessary about once a month. Satisfactory running conditions could usually be maintained in this way for periods of three or four months before it became necessary to open the apparatus for cleaning.

Only rough qualitative observations of the effects of such heating can be reported here since this apparatus is not suited to quantitative measurements of this nature. In general, heating was followed immediately by a period of very low detection efficiency for metastable atoms and relatively high efficiency for background radiation.[154] Conditions gradually returned to normal after several hours of reconditioning by exposure to a normal flow of hydrogen gas. In the absence of hydrogen, apparently no reconditioning occurred over a 24-hour period. Replacement of the tungsten detector plate by activated thoriated tungsten, zirconium, and platinum has in each case resulted in a satisfactory beam and there appears to be no qualitative basis for choice among these metals.

[153] See Part II, Sec. 43.

[154] See Part III, Sec. 67.

PHYSICAL REVIEW VOLUME 89, NUMBER 1 JANUARY 1, 1953

The Canonical Transformation for an Electron-Positron Field Coupled to a Time-Independent Electromagnetic Field*

H. E. Moses
Institute for Mathematics and Mechanics, New York University, New York, New York
(Received April 4, 1952)

The problem of the electron-positron field coupled to an unquantized electromagnetic field, constant in time, is solved in the Schrödinger picture by finding a suitable canonical transformation. It is shown that in the number representation this transformation satisfies an integro-difference equation which can be solved by means of a perturbation scheme in a manner analogous to the finding of one-particle canonical transformations. It is shown, moreover, that this canonical transformation can be expressed in terms of single-particle canonical transformations.

1. THE N REPRESENTATION OF THE ELECTRON-POSITRON FIELD

We consider the unperturbed energy representation of a single Dirac electron. A state is represented by a function of the momentum vector P, of the sign of the energy ϵ, and of the component of spin in the direction of momentum τ. These variables form a complete set of commuting variables. We shall designate this set of variables by the letter s and call s itself a "variable."

A state of the electron-positron field Φ is represented in the number representation (or Fock representation) by a set of functions $\psi_n(s)_n$, where $\psi_n(s)_n$ is an abbreviated expression for $\psi_n(s_1, s_2, \cdots, s_n)$ which is an antisymmetric function of the n variables $s_1, s_2, \cdots, s_n$. We call this representation "the N representation" and use the notation

$$\Phi \underset{N}{\leftrightarrow} \{\psi_n(s)_n\}. \tag{1}$$

The inner product of two states,

$$\Phi^{(1)} \underset{N}{\leftrightarrow} \{\psi_n{}^{(1)}(s)_n\}, \quad \Phi \underset{N}{\leftrightarrow} \{\psi_n(s)_n\},$$

is given by

$$(\Phi^{(1)}, \Phi) = \sum_{n=0}^{\infty} \int \cdots \int_{n\text{-fold}} \bar{\psi}_n{}^{(1)}(s_1, s_2, \cdots, s_n) \times \psi_n(s_1, s_2, \cdots, s_n) ds_1 ds_2 \cdots ds_n$$

$$\equiv \sum_{n=0}^{\infty} \int \bar{\psi}_n{}^{(1)}(s)_n \psi_n(s)_n (ds)_n, \tag{2}$$

where the integration over the variables $s_1, s_2, \cdots, s_n$ means integration over the continuous variables and summation over the discrete variables. The bar represents the complex conjugate. The annihilation operator $A^-(s')$ and creation operator $A^+(s')$ are defined by

* This work is an extract of a report for a project supported by the ONR and the Air Force Cambridge Research Center.